

Self-consistent analysis of hadron production in pp and AA collisions at mid-rapidity

G.I. Lykasov, A.I. Malakhov

Joint Institute for Nuclear Research, Dubna 141980, Moscow region, Russia

lykasov@jinr.ru
malakhov@ihe.jinr.ru

Abstract

The self-consistent approach based on similarity of inclusive spectra of hadrons produced in pp and AA collisions is reviewed. This approach allows us to describe rather well the ratio of proton to anti-proton yields in AA collisions as a function of the initial energy at a wide range from a few GeV to a few TeV. We suggest its modification due to the quark-gluon dynamics to describe the inclusive spectra of hadrons produced in pp collision as a function of the transverse momentum p_t at mid-rapidity. The extension of this approach to analyze the pion p_t -spectra produced in AA collision at high and middle energies and mid-rapidity is given. The satisfactory description of experimental data on these spectra in pp and AA collisions within the offered approach is shown.

1 Introduction

The similarity principle, for example, in physics is well known. Its application to the particle production in hadron-hadron collision has been proposed several decades ago by E.Fermi [1], I.Pomeranchuk [2], L.D.Landau [3] and R.Hagedorn [4, 5]. It was noticed that the transverse momentum spectra of the particles produced in these collisions had a universal form like $\rho_h \sim \exp(-m_{ht}/T)$, at least, at not large values of m_{ht} , where m_{ht} is the transverse mass of the produced hadron h and T is a constant dependent only of the type of final hadrons. There are many statistical models applied successfully a similar form to describe hadronic yields produced in heavy-ion collisions (see, for example, [6–8] and references therein). Actually, the parameter T is nothing to do the average transverse mass $\langle m_{ht} \rangle$. However, according to many experimental data, the average transverse momentum p_{ht} of the produced hadron or $m_{ht} = \sqrt{p_{ht}^2 + m_h^2}$ depends on the initial energy \sqrt{s} , especially at low \sqrt{s} . Here s is the energy squared in the c.m.s. of colliding particles and m_h is the mass of the produced hadron.

Almost all theoretical approaches operate with the relativistic invariant Mandelstam variables s, t, u to analyze the hadron inclusive spectra in the mid-rapidity region. As usual, the

spectra are presented in the factorized forms of two functions dependent of t or p_t^2 and s . However, there is another approach to analyze multiple hadron production in pp and AA collisions at high energies, which operates by using four velocities of the initial and final particles [9]. It is the so called “the self-similarity approach”, which demonstrates the similarity of inclusive spectra of hadrons produced in pp and AA collisions, as a function of similarity parameter Π . The approach of studying relativistic nuclear interactions in the four velocity space proved to be very fruitful [10]. In fact, this approach is valid not in the complete kinematical region. That will be discussed in our paper. The hadron inclusive spectra obtained within this approach are presented as a function of the relativistic invariant similarity parameter, which can be related to variables t and s , as it is shown in [11]. The general form of such spectrum is not factorized over t and s . In this paper we present further development of this approach and extend it to the hadron production in AA collisions at the center rapidity region.

2 The parameter or function of self-similarity Π .

The description of multi particle states of the relativistic nuclear physics in terms of macroscopic variables such as temperature, pressure, density, entropy, contradicts to an important principle, which is emphasized by Heisenberg [12]: physical laws and the approval must be expressed only within the observed values. In the study of collisions of the relativistic nuclei most of these macroscopic variables have not been observed. In this work we have used the approach based on the law of similarity which is applied in relativistic nuclear physics but not based on Lagrange method. This allows one to design the solution based on the above principles. In hydraulics, as it is well known, methods of the theory of dimensionality and similarity are widely used. In fact, the invariant relations between the measured parameters of the problem are determined. In hydrodynamics the methods of similarity are widely applied they often are the only mean of the equation analysis.

The versatility of the methods of similarity for the theory and experiment is not accidental. The fact is that similarity transformations define the invariant relationships which characterize the structure of all the laws of nature, including the laws of relativistic nuclear physics [13]. In analogy with the geometrical similarity for physical phenomena we have used invariant dimensionless combinations (similarity parameters), composed from the dimension values defining the task.

For example, when planning large expensive hydraulic structures it is necessary to carry out physical modeling. Geometrically, the body of model is made similarly to the nature-body. For the steady motion of a viscous incompressible fluid flowing over the body, the directions of the velocities in the model and nature are the same.

As the main parameters of the problem we have taken the following: l - the characteristic size of the body model, l^0 is the size of the nature body, l^0/l is the coefficient of geometric similarity, and U is the velocity of the impinging flow, μ is the viscosity of the fluid, ρ is the fluid density.

These parameters define the system of units: l - length, M - mass, T - time, and have the following dimensions:

$$[l] = L, [U] = L \cdot T^{-1}, [\mu] = M \cdot L^{-1} \cdot T, [\rho] = M \cdot L^{-3}.$$

From the defining parameters we can construct only one dynamic similarity parameter (a dimensionless combination, independent of the choice of measuring units):

$$\Pi = \rho U l / \mu = \text{Re}.$$

This invariant is called the Reynolds number. To provide the similarity, it is required to have equality of this parameter for the model and nature. If the distance \mathbf{r} is measured in units of l

and the velocity \mathbf{V} is measured in units of U , the solutions of the hydrodynamic equations for the velocity distributions will have the following form:

$$\mathbf{V}/U = \mathbf{f}(\mathbf{r}/l, \text{Re}).$$

From this expression it follows that the fields of the flow velocities around geometrically similar bodies are described by only one function, depending on \mathbf{r}/l if the Reynolds numbers for these flows are the same.

Within the self-similarity approach [9, 10] the predictions on the ratios of the particles produced in AA collisions at high energies were given in [13, 14]. Let us briefly present here the main idea of this study. Consider, for example, the production of hadrons 1, 2, etc. in the collision of nucleus I with nucleus II :



According to this assumption more than one nucleon in the nucleus I can participate in the interaction (1). The value of N_I is the effective number of nucleons inside the nucleus I , participating in the interaction which is called “the cumulative number”. Its values lie in the region of $0 \leq N_I \leq A_I$ (A_I - atomic number of nucleus I). The cumulative area complies with $N_I > 1$. Of course, the same situation will take place for the nucleus II , and it is possible to introduce the cumulative number of N_{II} .

For reaction (1) with the production of the inclusive particle 1 we can write the conservation law of four-momentum in the following form:

$$(N_I P_I + N_{II} P_{II} - p_1)^2 = (N_I m_0 + N_{II} m_0 + M)^2, \quad (2)$$

where N_I and N_{II} the number of nucleons involved in the interaction; P_I , P_{II} , p_1 are four momenta of the nuclei I and II and particle 1, respectively; m_0 is the mass of the nucleon; M is the mass of the particle providing the conservation of the baryon number, strangeness, and other quantum numbers.

In [13] the parameter of self-similarity is introduced, which allows one to describe the differential cross section of the yield of a large class of particles in relativistic nuclear collisions:

$$\Pi = \min\left[\frac{1}{2}[(u_I N_I + u_{II} N_{II})^2]\right]^{1/2}, \quad (3)$$

where u_I and u_{II} are four velocities of the nuclei I and II . The values N_I and N_{II} will be measurable, if we accept the hypothesis of minimum mass $m_0^2(u_1 N_1 + u_2 N_2)^2$ and consider the conservation law of 4-momentum. Thus, the procedure to determine N_I and N_{II} , and, hence, Π , is the determination of the minimum of Π on the basis of the conservation law of energy-momentum.

Then, it was suggested [13, 14] that the inclusive spectrum of the produced particle 1 in AA collision can be presented as the universal function dependent of the self-similarity parameter Π , which was chosen, for example, as the exponential function:

$$E d^3 \sigma / dp^3 = C_1 A_I^{\alpha(N_I)} \cdot A_{II}^{\alpha(N_{II})} \cdot \exp(-\Pi/C_2), \quad (4)$$

where $\alpha(N_I) = 1/3 + N_I/3$,
 $\alpha(N_{II}) = 1/3 + N_{II}/3$,
 $C_1 = 1.9 \cdot 10^4 \text{ mb} \cdot \text{GeV}^{-2} \cdot \text{c}^3 \cdot \text{st}^{-1}$ and
 $C_2 = 0.125 \pm 0.002$.

2.1 Relation of self-similarity function Π to the Mandelstam variables

s, t, u

As it is mentioned above, the exponential form for the hadron inclusive spectrum given by Eq.(4) was chosen as an example and using it we can satisfactorily describe the ratio of total yields of antiprotons to the protons produced in heavy nucleus-nucleus collisions. Unfortunately, this simple form Eq.(4) contradicts to the LHC data on the inclusive spectra of hadrons produced in the central pp collisions, as shown in [18]. Therefore, we use the results of [18] to present the inclusive relativistic invariant hadron spectrum at the mid-rapidity region and at not large hadron transverse momenta p_t in a more complicated form, which consists of two parts. The first one is due to the contribution of quarks, which was obtained within the QGSM (Quark-Gluon String Model) [19, 20] using the AGK (Abramovsky, Gribov, Kanchelli) cancellation [21] of n -pomeron exchanges for inclusive hadron spectra in the mid-rapidity region. It is written in the following form [18]:

$$E(d^3\sigma/d^3p)_q = \phi_q(y=0, p_t) \cdot \sum_{n=1}^{\infty} [n\sigma_n(s)] = \phi_q(y=0, p_t)g(s/s_0)^\Delta, \quad (5)$$

where $\sigma_n(s)$ is the cross-section to produce the n -pomeron chain (or $2n$ quark-antiquark strings); $g = 21$ mb - constant, which is calculated within the "quasi-eikonal" approximation [22]; $s_0 = 1$ GeV²; $\Delta = [\alpha_p(0) - 1] \sim 0.12$, where $\alpha_p(0)$ is the sub critical Pomeron intercept [19, 20, 22].

The second part of the hadron inclusive spectrum at the mid-rapidity region was introduced in [18, 23] assuming the contribution of the nonperturbative gluons and calculating it as the one-pomeron exchange between two nonperturbative gluons in the collided protons [23]. This part was written in the following form [18]:

$$\begin{aligned} E(d^3\sigma/d^3p)_g &= \phi_g(y=0, p_t) \cdot \sum_{n=2}^{\infty} (n-1)\sigma_n(s) \\ &= \phi_g(y=0, p_t) \cdot \left(\sum_{n=1}^{\infty} n\sigma_n(s) - \sum_{n=1}^{\infty} \sigma_n(s) \right) = \\ &\quad \phi_g(y=0, p_t) \cdot [g(s/s_0)^\Delta - \sigma_{nd}], \end{aligned} \quad (6)$$

where σ_{nd} is the non diffractive pp cross section.

Thus, taking into account the quark and gluon contributions we will get the following form for the inclusive hadron spectrum:

$$E(d^3\sigma/d^3p) = [\phi_q(y=0, p_t) + \phi_g(y=0, p_t) \cdot (1 - \sigma_{nd}/g((s/s_0)^\Delta))] \cdot g(s/s_0)^\Delta \quad (7)$$

The question arises, what is the relation of the similarity parameter Π to the relativistic invariant variables s, p_t^2 ? This relation can be found from Eqs.(21-24) using $ch(Y) = \sqrt{s}/(2m_0)$. Then, we have the following form for Π :

$$\Pi = \left\{ \frac{m_{1t}}{2m_0\delta} + \frac{M}{\sqrt{s}\delta} \right\} \left\{ 1 + \sqrt{1 + \frac{M^2 - m_1^2}{m_{1t}^2}} \delta \right\} \quad (8)$$

where $\delta = 1 - 4m_0^2/s$; $m_{1t} = \sqrt{p_t^2 + m_1^2}$ is the transverse mass of the produced hadron h . At

large initial energies $\sqrt{s} \gg 1$ GeV the similarity parameter Π becomes as following:

$$\Pi = \frac{m_{1t}}{2m_0(1 - 4m_0^2/s)} \left\{ 1 + \sqrt{1 + \frac{M^2 - m_1^2}{m_{1t}^2} (1 - 4m_0^2/s)} \right\} \quad (9)$$

For π -mesons $m_1 = \mu_\pi$ is the pion mass and $M = 0$; for K^- -mesons $m_1 = m_K$ is the kaon mass and $M = m_K$; for K^+ -mesons $m_1 = m_K$ and $M = m_\Lambda - m_0$, m_Λ is the mass of the Λ -baryon. For π -mesons at $p_t^2 \gg m_1^2$ we have:

$$\Pi \simeq \frac{m_{1t}}{m_0(1 - 4m_0^2/s)} \quad (10)$$

One can see that in the general case the similarity parameter Π depends on p_t^2 and s and asymptotically at large $s \gg 4m_0^2$ it depends only on $p_{t\pi}^2$. Let us stress that the dependence of Π on s is crucial at low initial energies only.

2.2 Quark-gluon dynamics of soft NN interaction and self-similarity function Π

The invariant inclusive spectrum can be also presented in the following equivalent form:

$$\rho_{NN} \equiv E_h \frac{d^3\sigma_{NN}}{d^3p_h} = \frac{1}{\pi} \frac{d\sigma}{dp_t^2 dy} \equiv \frac{1}{\pi} \frac{d\sigma}{dm_{1t}^2 dy} \quad (11)$$

Taking into account (11) we can rewrite Eq.(8) in the form:

$$\frac{1}{\pi} \frac{d\sigma_{NN}}{dm_{1t}^2 dy} = [\phi_q(y=0, \Pi) + \phi_g(y=0, \Pi) \cdot (1 - \sigma_{nd}/g((s/s_0)^\Delta))] \cdot g(s/s_0)^\Delta. \quad (12)$$

The first part of the inclusive spectrum (Soft QCD (quarks)) was calculated in [18, 23] within the QGSM [19, 20] and then, the function $\phi_q(y=0, \Pi)$ was fitted by the following form [11, 23]:

$$\phi_q(y=0, \Pi) = A_q \exp(-\Pi/C_q), \quad (13)$$

where $A_q = 3.68$ (GeV/c)⁻², $C_q = 0.147$ for $pp \rightarrow \pi X$ processes at the mid-rapidity and width region of initial energies.

The function $\phi_g(y=0, \Pi)$ related to the second part (Soft QCD (gluons)) of the spectrum, which was calculated in [23]. Then, for the pion production in pp collision at high energies it is fitted by the following form [11, 23]:

$$\phi_g(y=0, \Pi) = A_g \sqrt{m_{1t}} \exp(-\Pi/C_g), \quad (14)$$

where $A_g = 1.7249$ (GeV/c)⁻², $C_g = 0.289$.

Using (13) we can calculate the inclusive hadron spectrum as a function of the transverse mass.

In Fig. 1 the inclusive spectrum $(1/m_{1t})d\sigma/dm_{1t}dy$ of π^- -mesons produced in pp collisions at the initial momenta $P_{in} = 31$ GeV/c ($\sqrt{s} = 7.75$ GeV) per nucleon is presented versus their transverse mass m_{1t} . The similar satisfactory description of the NA61 data at $P_{in} = 158$ GeV/c ($\sqrt{s} = 17.29$ GeV) was obtained in our paper [11]. Using only the first part of the spectrum $\phi_q(y=0, m_{1t})$, which corresponds to the quark contribution, the conventional string model, let's call it the SOFT QCD (quarks), one can describe the NA61 data [24] rather satisfactorily at

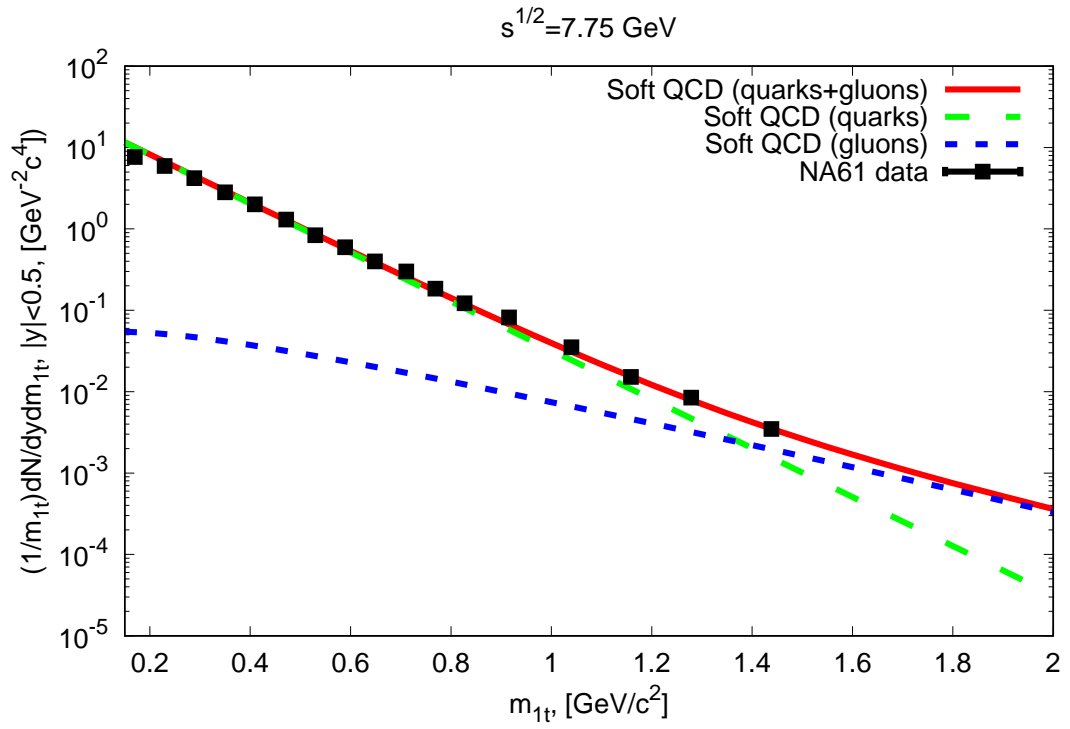


Figure 1: Results of the calculations of the inclusive cross section of pion production in pp collisions as a function of the transverse mass at $s^{1/2} = 7.75 \text{ GeV}$ or at the initial momentum $P_{in} = 31 \text{ GeV}/c$ in l.s.m. They are compared to the NA61 experimental data [24].

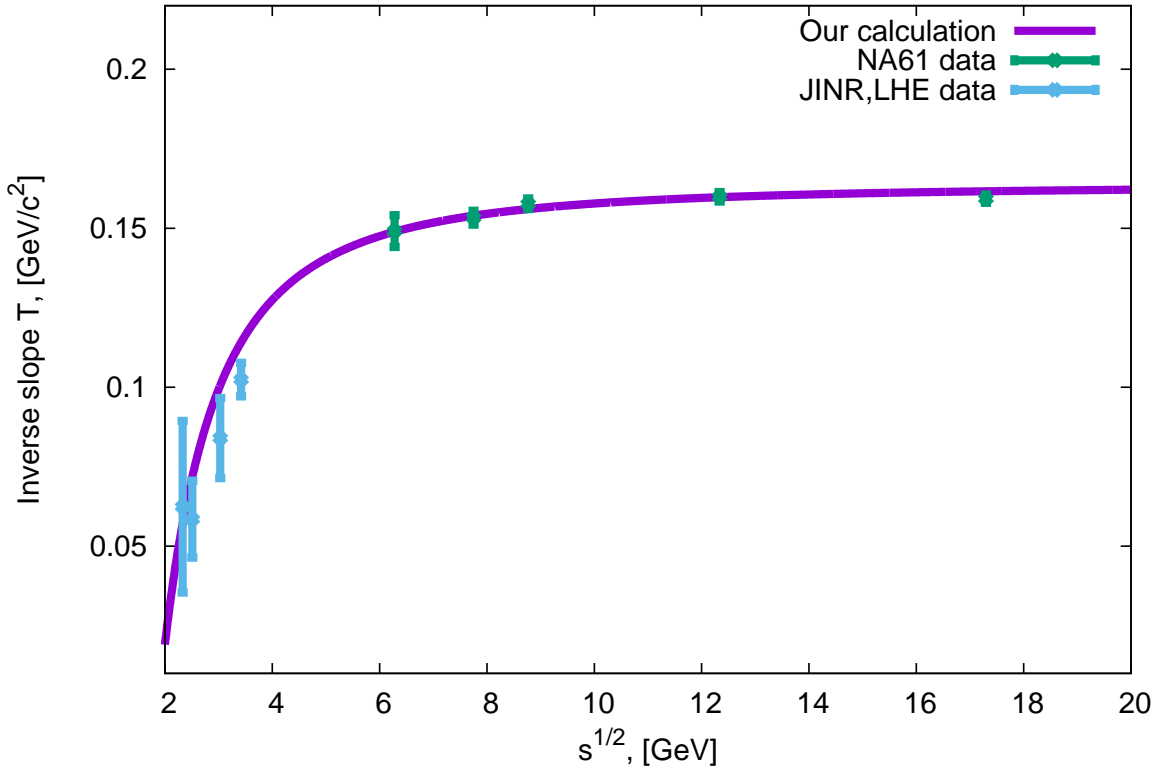


Figure 2: The inverse slope parameter T for the reaction $pp \rightarrow \pi^- X$ calculated using Eq. 16. The points at $6 \text{ GeV} < \sqrt{s} < 18 \text{ GeV}$ are the NA61 data [24], the points at $2 \text{ GeV} < \sqrt{s} < 4 \text{ GeV}$ are the data extracted from [25, 26].

$m_t < 1 \text{ GeV}/c^2$. This part of the inclusive spectrum corresponds to the dashed line in Fig. 1. The inclusion of the second part of spectrum due to the contribution of gluons (SOFT QCD (gluons)), the dotted line, allowed us to describe all the NA61 data up to $m_{1t} = 1.5 \text{ GeV}/c^2$, see the solid line in Fig. 1 (Soft QCD(quarks+gluons)). Actually, at large \sqrt{s} even at the NA61 energies $\Pi \simeq m_{1t}/m_0$ instead of (10). Generally the pion spectrum $\rho_{NN}(s, m_{1t} \equiv E_h(d^3\sigma/d^3p_h))$ (ignoring the gluon part) can be presented in the following approximated form, which is valid for the NA61 energies and low transverse momenta $p_t < 1 \text{ GeV}/c$:

$$\rho_{NN}(s, m_{1t}) \simeq \phi_q(y=0, \Pi)g(s/s_0)^\Delta = g(s/s_0)^\Delta \cdot A_q \exp\left(-\frac{m_{1t}}{C_q m_0(1 - 4m_0^2/s)}\right) \equiv g(s/s_0)^\Delta A_q \exp\left(-\frac{m_{1t}}{T}\right), \quad (15)$$

where

$$T = C_q m_0(1 - 4m_0^2/s) \quad (16)$$

is the inverse slope parameter, which is called sometimes as the *thermal freeze-out* temperature. One can see from Eq.(16) that this *thermal freeze-out* temperature depends on the initial energy square s in the c.m.s. of collided protons. That is the direct consequence of the self-similarity approach, which uses the four-momentum velocity formalism. This s -dependence of T is significant at low initial energies and at $s \gg m_0^2$ the inverse slope parameter T becomes independent on s . To describe rather well the NA61 data at larger values of p_t , the inclusive pion spectrum should be presented by Eq. (12). However, the main contribution to the inelastic total cross section comes from the first part of Eq.(12), which has the form given by Eq. (15). We have calculated the inverse slope parameter T for the pion production in pp collision as a function of the energy \sqrt{s} given by Eq.(16) and presented in Fig. 2. There is a good agreement

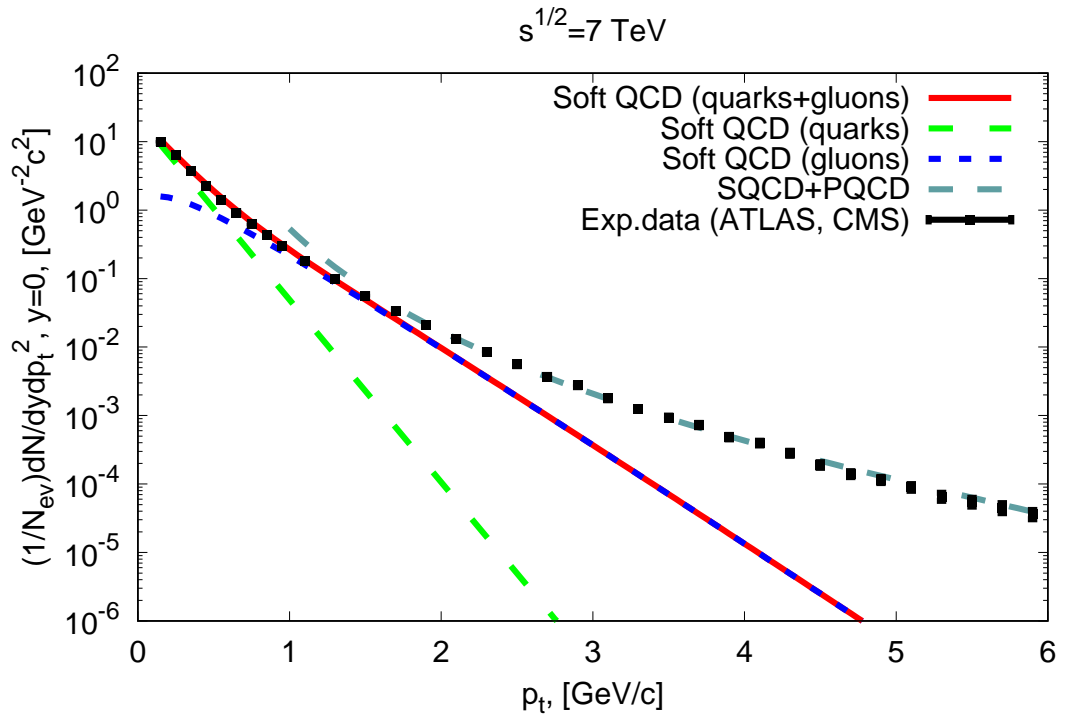


Figure 3: Results of the calculations of the inclusive cross section of charge hadrons produced in pp collisions at the LHC energies as a function of their transverse momentum p_t at $\sqrt{s} = 7 \text{ TeV}$. The points are the LHC experimental data [27, 28].

with the NA61 data [24] at $6 \text{ GeV} < \sqrt{s} < 18 \text{ GeV}$ and the JINR data [25,26] at $2 \text{ GeV} < \sqrt{s} < 4 \text{ GeV}$.

As, for example, in Fig. 3, we illustrate the satisfactory description of LHC data on inclusive spectrum of charged hadrons (mainly pions and kaons) at $\sqrt{s} = 7 \text{ TeV}$ by using Eq.(12) and the perturbative QCD (PQCD) within the LO [18, 23]. This spectrum is the sum of inclusive spectra of pions and kaons, therefore it is presented as a function of the transverse momentum p_t instead of functions of the transverse mass m_{1t} because the masses of a pion and kaon are different. In addition to the part of spectrum, which corresponds to Eq.(12), see the solid line in this figure, we also have included the PQCD calculations, see the dotted line. The PQCD calculations within the LO are divergent at low p_t , therefore, the dotted line goes up, when p_t decreases. The kinematical region about $p_t \simeq 1.8\text{-}2.2 \text{ GeV}/c$ can be treated as the matching region of the nonperturbative QCD (soft QCD) and the perturbative QCD (PQCD). One can see from Fig. (3) that it is possible to describe rather well these inclusive spectrum in the wide region of p_t at the LHC energies matching these two approaches. To describe rather well the LHC data on these inclusive p_t -spectra at $p_t > 2\text{-}3 \text{ GeV}/c$, the PQCD calculation should be included, whose contribution has a shape similar to the power law p_t -distribution [29]. Let us stress that the NA61 data and LHC ones on hadron transverse momentum spectra in pp collisions at the mid-rapidity region are described within our approach rather satisfactorily with $\chi^2/n.d.f. = 0.98$ [43].

3 Nucleus-nucleus collisions in the central rapidity region

The relativistic invariant inclusive spectrum of hadrons produced in AA collision in the central rapidity region and not large transverse momenta can be presented in the following form:

$$Ed^3\sigma_{AA}/dp^3 = C_1 A_I^{\alpha(N_I)} \cdot A_{II}^{\alpha(N_{II})} \cdot \rho_{NN}, \quad (17)$$

where ρ_{NN} is the inclusive relativistic invariant pion spectrum in pp collision given by Eq. (13), $\alpha(N) = 1/3 + N/3$, the s -dependent function N is calculated using Eqs. (21-24). The results of our calculations of p_t -spectra of pions produced in AA collisions in the central rapidity region and different high and middle energies compared to different experimental data are presented in Figs. (4-6). One can see from Fig. (4) that our approach is able to get a satisfactory description of the data on pion production in $AuAu$ and $PbPb$ collisions at the STAR and LHC energies as well as in $p - p$ collisions, see Figs. (1,2) at $p_t \leq 1.2 \text{ GeV}/c$. In principle, there can be another theoretical interpretation of multiple hadron production in heavy-ion collisions at high energies based, for example, on the stationary thermal model [30,31]. At middle initial energies about $1 \text{ GeV}\text{-}8 \text{ GeV}$ our calculations of pion p_t -spectra in heavy ion collisions, namely $AuAu$, $ArKCl$, at the central rapidities result in a more or less satisfactory description of the data shape at low $p_t < 0.5\text{-}0.6 \text{ GeV}/c$, as it also can be seen in Figs. (4-6). By calculation of all the pion p_t -spectra in AA collisions at mid-rapidity we used the same form of ρ_{NN} applied to the satisfactory description of the NA61 and LHC data on hadron production in pp collisions, see Figs. (4-6). The energy dependence of these spectra is given by the term $g(s/s_0)^\Delta$ for the quark contribution and the term $(g(s/s_0)^\Delta - \sigma_{nd})$ for the gluon contribution to ρ_{NN} . The non diffractive cross section σ_{nd} , as a difference between the total pp cross section σ_{tot} and the elastic (σ_{el}) and the diffractive (σ_{dif}) cross sections at high energies is taken from the experimental data. At middle energies about several GeV there are very poor data on the diffractive cross section σ_{dif} . Therefore, at \sqrt{s} about a few GeV our calculations are not so precise, as at high energies. As one can see from Fig.(4) the $m_{\pi t}$ -pion spectra in heavy ion collisions, as $Au + Au$, $Pb + Pb$, at high energies and the mid-rapidity are described rather satisfactorily within the proposed approach at $m_{\pi t} < 0.7 \text{ GeV}/c^2$ with $\chi^2/n.d.f. = 0.98$.

A small deviation of our calculations from the HADES data less than 10 % can be seen in the $m_{\pi\pi}$ -spectra of the pions produced in $Ar + KCl$ collision at the initial kinetic energies per nucleon about 1.75 GeV ($\sqrt{s} = 2.61$ GeV) and $m_{\pi\pi} < 0.6$ GeV/c² presented in Fig. 5 (right). It is illustrated by the Table 1 presented in the Appendix. Approximately the same deviation, as in the Table 1, is for the pion production in $Au + Au$ collision also at $m_{\pi\pi} < 0.6$ GeV/c², see Fig. 5 (right). However, at $m_{\pi\pi} > 0.6$ GeV/c² this deviation can be about 20%-70%, as it is seen from the Table 1.

Contrary to this the rather big deviation of our calculations from the HADES data is seen in the pion production in $C^{12} + C^{12}$ collision at the initial kinetic energy per nucleon about 2 GeV presented in Fig. 6 (left) especially at $m_{\pi\pi} > 0.3$ GeV/c². However, the AGS data for $Au + Au \rightarrow \pi + X$ reaction at the same energy per nucleon are described more better, as it is seen in Fig. 5 (left).

A big deviation of the theory from the data is not seen in p_T -spectra of the pions produced in heavy ion collisions, for example, $AuAu, PbPb$. It can be due to the difference between nuclear density $\rho_N(k)$ distribution in heavy nuclei and light nuclei. In the heavy nucleus $\rho_N(k)$ as function of the internal nucleon momentum k is more flat compared to the nucleon distribution in the light nucleus, therefore the pion production in heavy ion collision can be less sensitive to the nuclear structure compared to the same pion production in light nucleus-nucleus collisions.

In Fig. 6 (right) we present the prediction of pion $m_{\pi\pi}$ -spectrum in $AuAu$ collision in the mid-rapidity region and centrality about (0-5)% for the HADES experiment at initial kinetic energy per nucleon about 1.25 GeV ($\sqrt{s} = 2.42$ GeV).

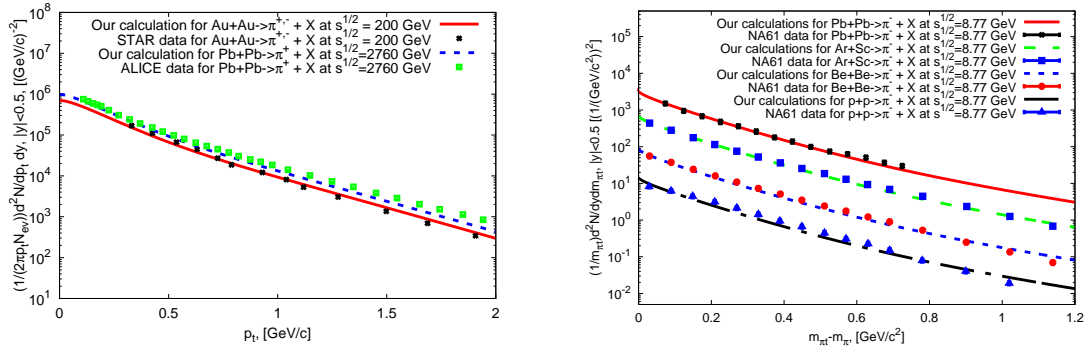


Figure 4: Left: results of our calculations of pion p_T -spectra in $AuAu$ and $PbPb$ collisions in the mid-rapidity region ($|y| < 0.5$) compared to the STAR [32, 33] and ALICE [34–37] data. Right: Results of our calculations of pion $m_{\pi\pi}$ -spectra in $PbPb, ArSc, BeBe$ and pp collisions at $\sqrt{s} = 8.77$ GeV or at the initial momentum per nucleon $P_{in} = 40$ GeV/c and the mid-rapidity region compared to the NA61 [38, 39] data.

4 Conclusion

The inclusive hadron spectrum in the space of four-velocities is presented within the self-similarity approach as a function of the similarity parameter Π . The use of the self-similarity approach allows us to describe the ratio of the total yields of protons to the anti-protons produced in AA collisions as a function of the energy in the mid-rapidity region and a wide energy range from 10 GeV to a few TeV [11].

We have shown that the energy dependence of the similarity parameter Π included within this approach is very significant at low energies, namely at $\sqrt{s} < 6$ GeV, and rather well repro-

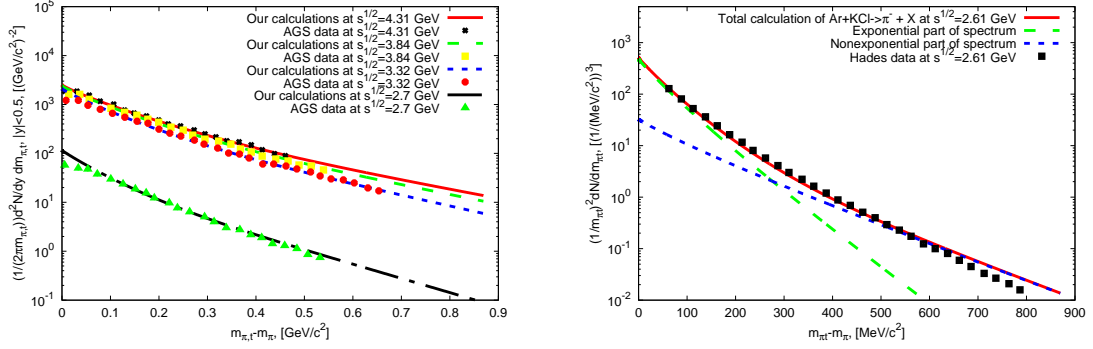


Figure 5: Left: our calculations of pion $m_{\pi t}$ -spectra in $AuAu$ collision in the mid-rapidity region at $\sqrt{s} = 4.31, 3.84, 3.32, 2.7$ GeV or the initial kinetic energies per nucleon about $E_{kin} = 8, 6, 4, 2$ GeV respectively. They are compared to the AGS data [40]. Right: results of our calculations of pion $m_{\pi t}$ -spectra in $ArKCl$ collision in the mid-rapidity region at $\sqrt{s} = 2.61$ GeV or at initial kinetic energy per nucleon about 1.75 GeV compared to the HADES data [41]; the long dash line corresponds to the exponential part of pion spectrum given by Eq.(13) and the short dash curve corresponds to the nonexponential part given by Eq.(14).

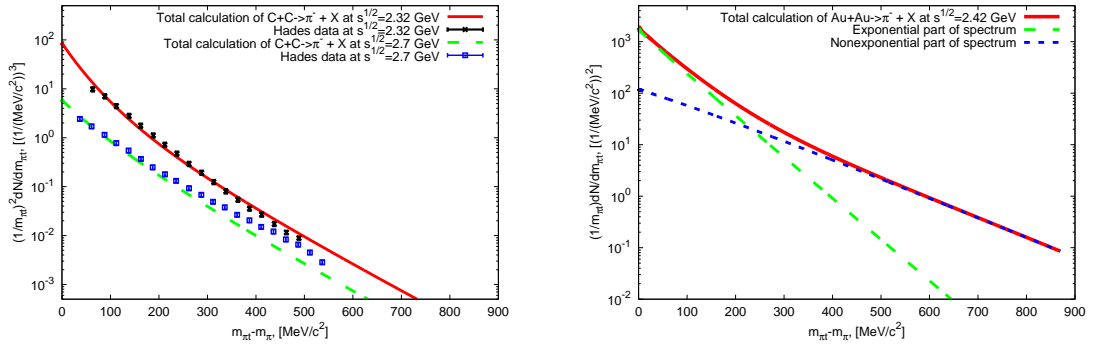


Figure 6: Left: results of our calculations of pion $m_{\pi t}$ -spectrum in $C^{12}C^{12}$ collision in the mid-rapidity at the initial kinetic energy per per nucleon about 1 GeV ($\sqrt{s} = 2.32$ GeV) and 2 GeV ($\sqrt{s} = 2.7$ GeV) compared to the HADES data [42]. Right: our predictions of pion $m_{\pi t}$ -spectrum in $AuAu$ collision in the mid-rapidity region or initial kinetic energy per nucleon about 1.25 GeV ($\sqrt{s} = 2.42$ GeV) at the centrality about (0-5)%; the long dash line corresponds to the exponential part of pion spectrum given by Eq.(13) and the short dash curve corresponds to the non exponential part given by Eq.(14).

duces the experimental data on the inverse slope or the *thermal freeze-out* temperature of the inclusive spectrum of the hadrons produced in pp collisions. The parameter Π increases and saturates when \sqrt{s} grows. This is very significant for a theoretical interpretation of the future experimental data planned to get at FAIR, CBM (Darmstadt, Germany), RHIC (BNL, Brookhaven, USA) and NICA (Dubna, Russia) projects. That is an advantage of the self-similarity approach compared to other theoretical models.

However, we have also shown that the s dependence of Π is not enough to describe the inclusive spectra of the hadrons produced in the mid-rapidity region, for example, in pp collisions in the wide region of initial energy, especially at the LHC energies. Therefore, we have modified the self-similarity approach using the quark-gluon string model (QGSM) [19, 20] and [18, 23] including the contribution of nonperturbative gluons, which are very significant to describe the experimental data on inclusive hadron spectra in the mid-rapidity region at the transverse momenta p_t up to 2-3 GeV/c [18, 23]. Moreover, the gluon density obtained in [23], whose parameters were found from the best description of the LHC data and also allowed us to describe the HERA data on the proton structure functions [43]. To describe the data in the mid-rapidity region and values of p_t up to 2-3 GeV/c, we have modified the simple exponential form of the spectrum, as a function of Π , and presented it in two parts due to the contribution of quarks and gluons, each of them has a different energy dependence. This energy dependence was obtained in [18] by using the Regge approach valid for soft hadron-nucleon processes. To extend the application of the offered approach to analyze these inclusive p_t -spectra at large hadron transverse momenta, we have to take the PQCD calculations into account.

This approach is applied to the analysis of pion production in pp , AA and pA collisions in the mid-rapidity region. We have shown the self-consistent satisfactory description of the data on p_t -spectra of the pions in these interactions in a wide region of initial energies and not large transverse momenta of pions. The approach suggested in this paper results in a more or less well description of these spectra for heavy-ion collisions. However, it can not be applied to the analysis of hadron production in light nucleus-nucleus collisions, especially, at middle energies because the production mechanism is very sensitive to the nuclear structure, which is different for heavy and light nuclei.

Acknowledgements.

We are very grateful to A.P. Jerusalimov, A.A. Baldin, A.V. Belayev, A.Yu. Troyan for giving us the experimental data obtained at the JINR. We thank M. Gumberidze, R. Holzmann, G. Kornakov, A. Rustamov, J. Stroth for extremely helpful discussions and very productive collaboration. We are also grateful to P. Braun-Munzenger, T. Galatyuk, V.P. Ladygin, M. Lorenz, V. Pechenov, B. Ramstein, P. Salapura for helpful discussions.

APPENDIX

In this paragraph we present the analytical form of the self-similarity function Π . Equation (2) can be written as follows:

$$N_I \cdot N_{II} - \Phi_I \cdot N_I - \Phi_{II} \cdot N_{II} = \Phi_M \quad , \quad (18)$$

where relativistic invariant dimensionless values have been introduced:

$$\begin{aligned} \Phi_I &= [(m_1/m_0) \cdot (u_I u_1) + M/m_0] / [(u_I u_{II}) - 1] \\ \Phi_{II} &= [(m_1/m_0) \cdot (u_{II} u_1) + M/m_0] / [(u_I u_{II}) - 1] \\ \Phi_M &= (M^2 - m_1^2) / [2m_0^2((u_I u_{II}) - 1)]. \end{aligned}$$

Equation (18) can be written as follows:

$$[(N_I/\Phi_{II}) - 1] \cdot [(N_{II}/\Phi_I) - 1] = 1 + [\Phi_M/(\Phi_I \cdot \Phi_{II})]. \quad (19)$$

Minimum Φ is found from the following:

$$d\Pi/dN_I = 0, \quad d\Pi/dN_{II} = 0. \quad (20)$$

Let us introduce the intermediate variables:

$$F_I = [(N_I/\Phi_{II}) - 1], \quad F_{II} = [(N_{II}/\Phi_I) - 1].$$

From the above we obtain: $F_I \cdot F_{II} = 1 + \Phi_M/(\Phi_I \cdot \Phi_{II})$.

Then, (20) is also equal to 0 as

$$d\Pi/dF_I = 0, \quad d\Pi/dF_{II} = 0.$$

From (3) we can obtain:

$$\begin{aligned} 4\Pi^2 &= N_I^2 + N_{II}^2 + 2N_I \cdot N_{II} \cdot (u_I u_{II}), \\ 4\Pi^2 &= (F_I + 1)^2 \Phi_{II}^2 + (F_{II} + 1)^2 \Phi_I^2 + \\ &2\Phi_I \cdot \Phi_{II} (F_I + 1) \cdot (F_{II} + 1) \cdot (u_I u_{II}) F_{II} = \alpha/F_I. \end{aligned}$$

The condition of the minimum $d(4\Pi^2)/dF_I = 0$ gives the equation for F_I :

$$\begin{aligned} F_I^4 + F_I^3 - (\Phi_I/\Phi_{II})^2 \cdot (\alpha^2 + \alpha F_I) + (u_I u_{II}) \cdot \\ (\Phi_I/\Phi_{II}) \cdot (F_I^3 - \alpha F_I) = 0 \end{aligned}$$

or

$$\begin{aligned} F_I^4 + F_I^3 [1 + (u_I u_{II})/z] - (\alpha/z) \cdot F_I \cdot [(u_I u_{II}) + \\ (1/z)] - \alpha^2/z^2 = 0, \end{aligned}$$

where $z = \Phi_{II}/\Phi_I$. Changing I to II we should replace $z \rightarrow (1/z)$, $F_I \rightarrow (\alpha/F_{II})$.

$$\begin{aligned} (\alpha/F_{II})^4 + (\alpha/F_{II})^3 [1 + (u_I u_{II})z] - \alpha z (\alpha/F_{II}) \cdot \\ [(u_I u_{II}) + z] - \alpha^2 z^2 = 0 \end{aligned}$$

or

$$F_{II}^4 + F_{II}^3 [1 + (u_I u_{II})z] - z\alpha \cdot F_{II} \cdot [z + (u_I u_{II})] - \alpha^2 z^2 = 0.$$

Thus, at $z = 1 \rightarrow F_I = F_{II}$, $\Phi_I = \Phi_{II} = \Phi$.

Since $F_I = F_{II}$, then $(N_I/\Phi - 1) = (N_{II}/\Phi - 1)$ and $N_I = N_{II}$.

$F^2 = \alpha$ and $F_I = F_{II} = \alpha^{1/2} = [1 + (\Phi_M/\Phi^2)]^{1/2}$.

$$\begin{aligned} N_I = N_{II} = N = (1 + F)\Phi = \\ \{1 + [1 + (\Phi_M/\Phi^2)]^{1/2}\}\Phi \end{aligned} \quad (21)$$

$$\begin{aligned} \Pi = 1/2[2N^2 + 2N^2(u_I u_{II})]^{1/2} = \\ N/\sqrt{2}[1 + (u_I u_{II})] = N \cdot chY. \end{aligned} \quad (22)$$

Note that $(u_I u_{II}) = ch2Y$, $(u_I u_1) = (m_t/m_1) \cdot ch(-Y - y) = (m_t/m_1) \cdot ch(Y + y)$ and $(u_{II} u_1) = (m_t/m_1) \cdot ch(Y - y)$. Here m_t is the transverse mass of the particle 1, $m_t = (m_1^2 + p_t^2)^{1/2}$, Y - rapidity of interacting nuclei, y - particle 1 rapidity. At $y = 0$ (in the central rapidity region) we obtain the following:

$$(u_I u_1) = (u_{II} u_1) = (m_{1t}/m_1) \cdot chY, \quad m_{1t} = (m_1^2 + p_t^2)^{1/2}$$

$$\Phi = (1/m_0) \cdot (m_{1t} chY + M) \cdot [1/(2sh^2 Y)] \quad (23)$$

$$\Phi_M = (M^2 - m_1^2)/(4m_0^2 sh^2 Y) \quad (24)$$

References

- [1] E. Fermi, Phys. Rev. **92**, (1953) 452.
- [2] I. Ya. Pomeranchuk, Izv. Dokl. Akad. Nauk Ser.Fiz. **78** (1951) 889.
- [3] L.D. Landau, Izv. Akad. Nauk Ser. Fiz. **17** (1953) 51.
- [4] R. Hagedorn, Supplemento al Nuovo Cimento **3**, 147 (1965).
- [5] P. Braun-Munzinger, K. Redlich, J. Stachel, Nucl.Phys. **A904** (2013) 535c.
- [6] S. Chatterjee et al., Advances in High Energy Physics, vol.2015, ID 349013.
- [7] K.A. Bugaev et al., Nucl.Phys. **A970** (2018) 133.
- [8] A. Andronic, P. Braun-Munzinger, J. Stachel, Nucl. Phys. **A772** (2006) 167; arXiv:0511071 [nucl-th].
- [9] A.M. Baldin, L.A. Didenko, Fortsch.Phys. **38** (1990) 261.
- [10] A.M. Baldin, A.I. Malakhov, and A. N. Sissakian, Phys. Part. Nucl. **29** (Suppl. 1) (2001), 4.
- [11] D.A. Artemenkov, G.I. Lykasov, A.I. Malakhov, Int.J.Mod.Phys. **A30** (2015) 1550127.
- [12] W. Heisenberg, Physik und Philosophie, Frankfurt am Main, 1959.
- [13] A.M. Baldin and A.A. Baldin. Physics of Particles and Nuclei **29**, 1998, 232.
- [14] A.M. Baldin, A.I. Malakhov, JINR Rapid Communications 1 [87]-98 (1998) 5.
- [15] A. Tawfik, Nuclear Physics **A859**, (2011) 63.
- [16] <http://hepdata.cedar.ac.uk/view/p7907>.
- [17] R. Klingenberg *et al.*, Nuclear Physics **A610**, (1996) 306c.
- [18] V.A. Bednyakov, A.A. Grinyuk, G.I. Lykasov, M. Pogosyan; Int.J.Mod.Phys. **A27** (2012) 1250042.
- [19] A.B. Kaidalov, Z.Phys. **C12**, (1982) 63.
- [20] A.B. Kaidalov, Surveys High Energy Phys. **13**, (1999) 265.
- [21] V. Abramovsky, V. N. Gribov and O. Konchelli, Sov.J.Nucl.Phys. **18**, (1973) 308.
- [22] K.A. Ter-Martirosyan, Sov.J.Nucl.Phys., **44**, (1986) 817
- [23] A.A. Grinyuk, G.I. Lykasov, A.V. Lipatov, N.P. Zotov, Phys.Rev. **D87**, (2013) 074017.
- [24] A.A. Abgrall *et al*, Eur.Phys.J., **C74**, (2014) 2794.
- [25] A.P. Jerusalimov *et al.*, Eur.Phys.J. **A51**, 83 (2015).
- [26] A.P. Jerusalimov, *et al.*, EPJ Web Conf. **138**, 07008, (2017).
- [27] V. Khachatryan, *et al.*, (CMS Collaboration), Phys. Rev. Lett. **105**, (2010) 022002.

- [28] G. Aad, *et al.*, (ATLAS Collaboration), *New J. Phys.* **13**, (2011) 053033.
- [29] J. Cleymans, G.I. Lykasov, A.S. Parvan, A.S. Sorin, O.V. Teryaev, *Phys.Lett.* **B723**, (2013) 351; arXiv:1302.1970 [hep-ph].
- [30] E. Schnedermann, U. Heinz, *Phys.Rev.* **C47**, 1738 (1993).
- [31] E. Schnedermann, J. Solfrank, U. Heinz, *Phys.Rev.* **C48**, 2462 (1993).
- [32] B.I. Abelev *et al.*, (STAR Collaboration), *Phys. Rev.* **C75**, 064901 (2007).
- [33] B.I. Abelev *et al.*, (STAR Collaboration), *Phys.Rev.Lett.*, **97**, 152301 (2006).
- [34] K. Aamodt, *et al.*, (ALICE Collaboration), *Eur. Phys. J. C* **71** 1655 (2011).
- [35] K. Aamodt, *et al.*, (ALICE Collaboration), *Phys. Lett.* **B693**, 53 (2010).
- [36] K. Aamodt, *et al.*, (ALICE Collaboration), *Phys. Rev.* **D82**, 052001 (2010).
- [37] K. Aamodt, *et al.*, (ALICE Collaboration), *Phys. Rev.* **C88**, 044910 (2013).
- [38] E. Kaptur, *PoS CPOD2014*, (2015) 053
- [39] M. Lewicki, arXiv:1612.01334 [hep-ex].
- [40] J.L. Klay, *et all*, (AGS Collaboration), *Phys.Rev.* **C68**, (2003) 054905
- [41] P. Tlusty, *et all.*, (HADES Collaboration), arXiv:0906.2309 [nucl-ex].
- [42] G. Agakishv, *et all.*,(HADES Collaboration), *Eur.Phys.J.*, **A40**, (2009) 45.
- [43] A.V. Lipatov, G.I. Lykasov, N.P. Zotov, *Phys.Rev.* **D89**, (2014) 014001.

$m_{\pi t} - m_{\pi}$ MeV/c ²	Theory (MeV/c ²) ⁻³	Exp. data (MeV/c ²) ⁻³
6.259e+01	1.297e+02	1.278e+02
8.819e+01	7.958e+01	8.066e+01
1.124e+02	4.949e+01	5.248e+01
1.380e+02	3.270e+01	3.631e+01
1.622e+02	2.173e+01	2.436e+01
1.878e+02	1.456e+01	1.634e+01
2.134e+02	9.870e+00	1.166e+01
2.361e+02	7.045e+00	8.066e+00
2.617e+02	4.954e+00	5.754e+00
2.873e+02	3.506e+00	4.105e+00
3.101e+02	2.622e+00	3.020e+00
3.371e+02	1.881e+00	2.222e+00
3.613e+02	1.421e+00	1.634e+00
3.869e+02	1.067e+00	1.202e+00
4.111e+02	8.215e-01	8.844e-01
4.367e+02	6.283e-01	6.918e-01
4.623e+02	4.844e-01	5.089e-01
4.879e+02	3.761e-01	3.981e-01
5.121e+02	2.992e-01	2.929e-01
5.377e+02	2.349e-01	2.291e-01
5.619e+02	1.886e-01	1.738e-01
5.875e+02	1.499e-01	1.240e-01
6.117e+02	1.211e-01	1.000e-01
6.373e+02	9.642e-02	8.066e-02
6.615e+02	7.826e-02	5.934e-02
6.856e+02	6.363e-02	4.501e-02
7.127e+02	5.053e-02	3.311e-02
7.368e+02	4.120e-02	2.671e-02
7.639e+02	3.294e-02	2.089e-02
7.866e+02	2.725e-02	1.585e-02

Table 1: Our calculations of the pion spectrum $(1/m_{\pi t})^2 dN/dm_{\pi t}$ presented in Fig. 5 as a function of $m_{\pi t} - m_{\pi}$ (MeV/c²) in *ArKCl* collision at the mid-rapidity region and initial kinetic energy per nucleon about 1.75 GeV ($\sqrt{s} = 2.61$ GeV), second column, compared to the HADES data [41] (third column).